

Passive acoustic tracking using a library of nearby sources of opportunity

Christopher M. A. Verlinden, J. Sarkar, W. S. Hodgkiss, W. A. Kuperman, and K. G. Sabra

Citation: *The Journal of the Acoustical Society of America* **143**, 878 (2018); doi: 10.1121/1.5022782

View online: <https://doi.org/10.1121/1.5022782>

View Table of Contents: <https://asa.scitation.org/toc/jas/143/2>

Published by the *Acoustical Society of America*

ARTICLES YOU MAY BE INTERESTED IN

Passive acoustic source localization using sources of opportunity

The Journal of the Acoustical Society of America **138**, EL54 (2015); <https://doi.org/10.1121/1.4922763>

Head waves in ocean acoustic ambient noise: Measurements and modeling

The Journal of the Acoustical Society of America **143**, 1182 (2018); <https://doi.org/10.1121/1.5024332>

Multiple-array passive acoustic source localization in shallow water

The Journal of the Acoustical Society of America **141**, 1501 (2017); <https://doi.org/10.1121/1.4976214>

Underwater acoustic source localization using generalized regression neural network

The Journal of the Acoustical Society of America **143**, 2321 (2018); <https://doi.org/10.1121/1.5032311>

Source localization using deep neural networks in a shallow water environment

The Journal of the Acoustical Society of America **143**, 2922 (2018); <https://doi.org/10.1121/1.5036725>

Determination of acoustic waveguide invariant using ships as sources of opportunity in a shallow water marine environment

The Journal of the Acoustical Society of America **141**, EL102 (2017); <https://doi.org/10.1121/1.4976112>

The advertisement features a white header with the text "COMSOL Day" in large blue letters, with "Acoustics" in smaller blue letters below it. To the right, a dark blue background contains white text: "A free, online event where you can attend multiphysics simulation sessions, ask COMSOL staff your questions, and more". Below this text is a red button with the white text "JOIN US MAY 25 >". To the right of the text is a 3D visualization of a submarine in an ocean environment, with a circular pattern of colored arrows (blue, green, yellow, red) indicating acoustic or simulation data around it.

Passive acoustic tracking using a library of nearby sources of opportunity

Christopher M. A. Verlinden,^{a)} J. Sarkar, W. S. Hodgkiss, and W. A. Kuperman
Scripps Institution of Oceanography, University of California San Diego, 9500 Gilman Drive, La Jolla, California 92093-0238, USA

K. G. Sabra
Mechanical Engineering Department, Georgia Institute of Technology, 801 Ferst Drive, Georgia Institute of Technology, Atlanta, Georgia 30332 0405, USA

(Received 3 July 2017; revised 15 December 2017; accepted 12 January 2018; published online 13 February 2018)

A method of localizing unknown acoustic sources using data derived replicas from ships of opportunity has been reported previously by Verlinden, Sarkar, Hodgkiss, Kuperman, and Sabra [J. Acoust. Soc. Am., **138**(1), EL54–EL59 (2015)]. The method is similar to traditional matched field processing, but differs in that data-derived measured replicas are used in place of modeled replicas and, in order to account for differing source spectra between library and target vessels, cross-correlation functions are compared instead of comparing acoustic signals directly. The method is capable of localizing sources in positions where data derived replicas are available, such as locations previously transited by ships tracked using the Automatic Identification System, but is limited by the sparsity of ships of opportunity. This paper presents an extension of this localization method to regions where data derived replicas are not available by extrapolating the measured cross-correlation function replicas onto a larger search grid using waveguide invariant theory. This new augmentation provides a method for continuous tracking.

© 2018 Acoustical Society of America. <https://doi.org/10.1121/1.5022782>

[BTH]

Pages: 878–890

I. INTRODUCTION

Passive acoustic source localization methods, such as matched field processing (MFP)¹ break down because of the difficulty in modeling the acoustic environment in the ocean with sufficient precision to generate modeled replicas accurate enough to consistently localize targets. The method presented in Verlinden *et al.*² addresses this issue by using measured replica fields, rather than modeled replica fields, in a localization scheme similar to MFP. This type of measured replica field MFP had been demonstrated previously using an active acoustic source of known characteristics by Fialkowski *et al.*³ In Verlinden *et al.*,² the library is instead populated using replicas generated by ships, used as acoustic sources of opportunity, and the difference in source spectra between different ships is overcome by using the cross-correlation of the acoustic signal on two arbitrarily horizontally separated hydrophones, rather than the signal itself. The cross-correlation is dependent on the arrival structure of the incoming signal, and is therefore a function of the position of the radiator and characteristics of the waveguide, and is independent of source spectra.⁴

The theory developed by Verlinden *et al.*² was demonstrated using numerical simulations for the case of a fully populated library and validated using experimental data for discrete locations populated with measured replicas. A grid is populated with measured replica cross-correlation

functions computed across two horizontally separated hydrophones using the acoustic signals from ships tracked using the Automatic Identification System (AIS).² Contacts are localized by comparing the library of measured replica cross-correlation functions to the cross-correlation function computed across the same two hydrophones, in the presence of an acoustic radiator in an unknown position, and assigning the location corresponding to the closest match between replica and data to the target vessel.² This method is necessarily limited by the inherent sparsity of ship traffic, in that replicas will only exist in areas transited by vessels. This motivates the need for an interpolation scheme designed to fill in the gaps between existing measured library replicas, in order to positively localize contacts in all locations, and continuously track moving targets.

This paper describes the environmental acoustic formulation for such an interpolation scheme, demonstrates the theory using numerical simulations, and validates those simulations using data gathered from an acoustic field experiment conducted off the coast of San Diego, CA. The method presented here allows for continuous tracking of contacts in the experiment area. The experiment was conducted in 150 m of water, 20 km off the coast of San Diego, CA. There was a strongly downward refracting sound speed profile as shown in Fig. 1(a) that was fairly stable for the ten days experiment conducted in January–February, 2009. For the purposes of this demonstration, only a single hydrophone from each of two 16-element vertical line arrays (VLAs) was required. The VLAs were horizontally separated by 511 m and located 18 m off the bottom. The method requires

^{a)}Electronic mail: cmverlin@ucsd.edu

only two individual hydrophones, but arrays of hydrophones can be combined to improve signal-to-noise ratio (SNR) and enhance the method, provided the aperture of the array is such that the entire propagation cone, meaning sound propagating at angles less than the critical angle, is included in the broadside beam. It may be possible to extend this method to localize sub-surface sources using libraries derived from surface sources, but this demonstration focuses on the localization of surface sources in a high SNR environment. Localizing surface and semi-submersible acoustic targets at or near the surface is of interest to the Navy and Coast Guard for defense and law enforcement applications. Ships in the vicinity of the hydrophones were tracked using AIS data obtained from the United States Coast Guard Navigation Center (USCG NAVCEN).

In the previously reported literature,² it is possible to detect target vessels only in discrete locations where they cross the tracks of library vessels. In order to continuously track a target acoustic radiator, it is necessary to fully-populate a grid with measured replicas. Populating the region between measured replica functions requires

extrapolation of the time-domain cross-correlation functions in the library to different locations in range and azimuth distributed in the horizontal plane. To do so, replica cross-correlation functions at known bearing and ranges can be modified to estimate the cross-correlation function at a different bearing and range using the formulation described next.

II. THEORY

In the scenario of interest, when a vessel transits through the search grid, the acoustic signal on two horizontally separated hydrophones is recorded and cross-correlated. These time domain cross-correlation functions are saved as “measured replicas” for the location of the library vessel, as determined by AIS, at the time the cross-cross correlation function is computed. In the future when an unknown “target” acoustic source transits the experiment site, it is possible to determine when and where it crosses the paths of all previously recorded library vessels by comparing the envelope of the cross-correlation function computed during the

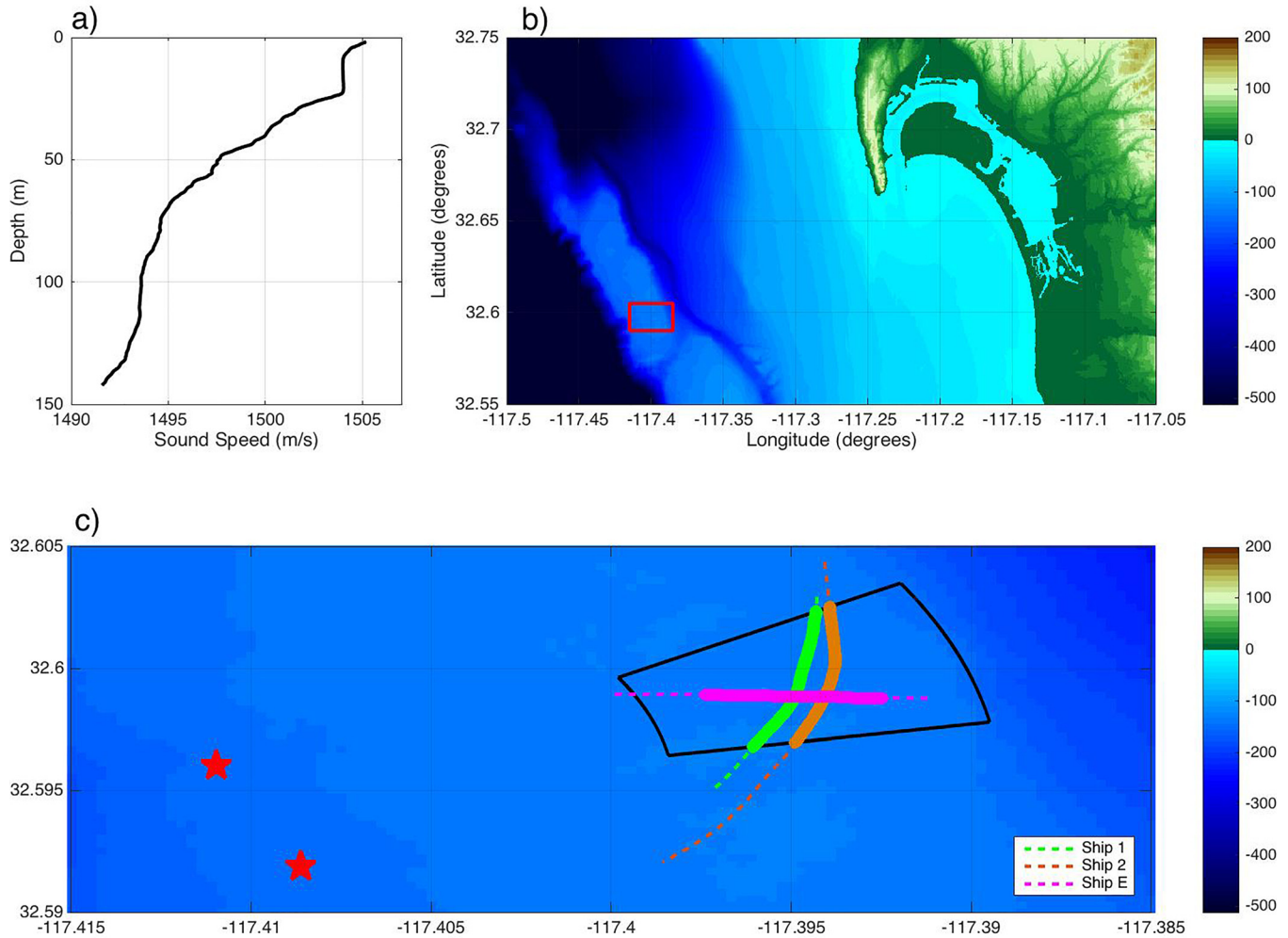


FIG. 1. (Color online) Experiment setup. The experiment was conducted in 150m of water with a strongly downward refracting sound speed profile (a) approximately 20km off the coast of San Diego, California. (b) shows the bathymetry in the vicinity of the hydrophones used in this experiment with a red box indicating the experiment site. The orange and green colored lines in (c) indicate ship tracks used to create the library of cross-correlation functions used to localize the target vessel plotted in magenta. The red stars indicate the location of the hydrophones which were used for the experiment. The black box represents the grid for which the library of replica cross-correlation functions was created and is the area shown in the localization ambiguity surfaces in Fig. 6.

transit of the target vessel with the envelopes of all the measured replica cross-correlation functions in the library.² The location with the replica that most closely resembles the cross-correlation function recorded during the transit of the target vessel, determined using the correlation coefficient between target and library cross-correlation function envelopes, is the location of the target vessel. The library cross-correlation functions must be extrapolated in order to fill in the gaps in coverage of measured replicas in order to allow for continuous tracking.

A. Formulation for fully populated library of replicas

The algorithm for extrapolating the cross-correlation functions is described schematically in Fig. 2. The blue “×” represents a location where a measured replica exists, computed by cross-correlating the acoustic signal on two horizontally separated hydrophones or arrays of hydrophones. The orange “×” represents a point in the search grid that needs to be populated by extrapolating the library cross-correlation function from the known location at angle θ , relative to the array azimuth and range R to the array center to some new angle $\theta + \Delta\theta$ and new range $R + \Delta r$. The array spacing is $2d$, the range to each hydrophone is r_1 and r_2 . Measured cross-correlation replica functions exist in all discrete locations that have been populated by a ship as a source of opportunity; the goal is to populate the entire search

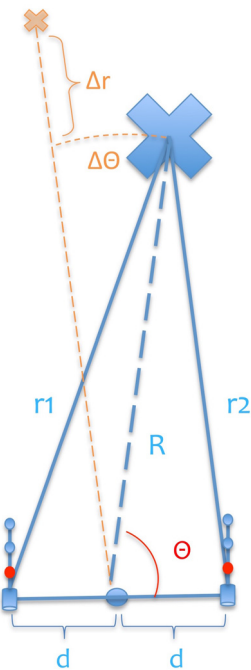


FIG. 2. (Color online) Schematic of extrapolation method with variables from Eqs. (1)–(6) labeled. The hydrophones (or arrays of hydrophones) are depicted as strings of dots with a cylindrical base. The distance between the hydrophones is $2d$; in this experiment 511 m. An existing measured cross-correlation function exists at the location depicted by the large blue “×,” which is a distance of r_1 meters from hydrophone 1, r_2 meters from hydrophone 2, R meters from the array center position, and angle θ relative to the array azimuth. The goal is to extrapolate the measured replica to the location shown by the small orange “×” at angle $\theta + \Delta\theta$, and range $R + \Delta r$, with the ultimate goal being to extrapolate the measured replica cross-correlation function at the blue “×” to all locations in the search grid.

region with estimated replica cross-correlation functions that have been extrapolated from the measured replicas. This is similar to shifting the focal range of a time reversal mirror by shifting signals in frequency as discussed in Kim *et al.*⁵ and is related to the source ranging methods discussed in Thode.⁶

Extrapolation of measured cross-correlation functions is accomplished by frequency shifting the waveform by some value ($\Delta\omega$) determined using the waveguide invariant (WGI), and multiplying the frequency shifted correlation function by a complex exponential, derived in the Appendix, as shown in Eqs. (1) and (4),

$$C(R + \Delta r, \theta + \Delta\theta, \omega) \approx C(R, \theta, \omega + \Delta\omega) \cdot \mathbf{F}(\Delta\theta, \Delta\omega), \quad (1)$$

where C represents the frequency domain cross-correlation function (i.e., cross spectra), R represents the range to the array center, Δr represents the difference in range to the new point in the library grid, θ represents the angle from the array azimuth to the location of the measured replica, $\Delta\theta$ represents the angle to be shifted or extrapolated, ω is the angular frequency of the cross spectra, and $\Delta\omega$ is the frequency shift needed to approximate the acoustic intensity of a signal at the range $R + \Delta r$ as defined by the WGI (β) in Eq. (2), and \mathbf{F} represents the complex exponential used to modify the correlation function in range and angle, which will be defined in this section and derived in the Appendix.

The WGI is a property which describes acoustic intensity fluctuations in range and frequency.^{7–10} It is defined as the ratio of the change in the modal group slowness with respect to the change in the modal phase slowness, and therefore encapsulates the dispersive characteristics of the waveguide into a single scalar parameter.¹¹ The interference pattern created by constructively and destructively interacting modes creates lines of constant intensity in range-frequency space for a waveguide of given characteristics. The WGI is a parameter which describes the slope of these lines at given ranges between source and receiver at given frequencies by the relationship defined in Eq. (2),

$$\beta = \left(\frac{r}{\omega} \right) \left(\frac{\Delta\omega}{\Delta r} \right) = - \frac{d(1/v_m)}{d(1/u_m)}, \quad (2)$$

$$\Delta\omega = \beta \frac{\omega}{r} \Delta r, \quad (3)$$

where β represents the WGI; r is the range from source to receiver; ω is the angular frequency; u_m is the modal group velocity; and v_m is the modal phase velocity. In many applications, the WGI is assumed to be one for a shallow water downward refracting environment such as the one used in this demonstration, illustrated in Fig. 1. That was not sufficient for the purposes of this localization method; the spatial variations in the WGI had to be accounted for.¹² For the purposes of this experiment, the WGI was measured experimentally, using ships as sources of opportunity, for each hydrophone, using the methods from Verlinden *et al.*¹² to create a map of β for the study area. Each grid point in the experiment area was assigned a β value for each hydrophone, which accounts for the propagation physics between

that point and the hydrophone. This value was determined by measuring the slope of intensity striations in range-frequency space as described in Verlinden *et al.*¹² A map of β values for this experiment area on one of the hydrophones used in this demonstration are published in Verlinden *et al.*¹²

Equation (4) is the formulation for F in the frequency domain,

$$F(\Delta\theta, \Delta\omega) = e^{-2i\bar{s}d\Delta\omega\cos(\theta+\Delta\theta)} e^{-2i\bar{k}d\Delta\theta\sin(\theta)}, \quad (4)$$

where \bar{k} represents the average horizontal modal wavenumber, and \bar{s} represents the average modal group slowness or the reciprocal of modal group speed. In simulations, \bar{k} and \bar{s} can be modeled; in practice these parameters are estimated using ships as sources of opportunity. Initial estimates of \bar{k} and \bar{s} are made using a standard normal mode propagation model for the acoustic environment used for the experiment, then these estimates are used to constrain a simple inversion for \bar{k} and \bar{s} using the localization formulation described in Eq. (7), and a library vessel in a known location transiting across the experiment area; adjusting \bar{k} and \bar{s} until the ship is localized in the proper location. The \bar{k} and \bar{s} values obtained using this method appear to be stable parameters of the waveguide, independent of source spectra. The derivations for Eq. (1) and Eq. (4) are included in the [Appendix](#).

As an aside, there are two special cases of this formulation. If sufficient library vessel tracks are available and measured replicas exist at all ranges, then the measured replica cross-correlation functions need only be extrapolated in angle and the formulation simplifies to

$$C(R, \theta + \Delta\theta) = C(R, \theta) e^{-2i\bar{k}d\Delta\theta\sin\theta}, \quad (5)$$

at the limit where Δr approaches zero in Eq. (1) and the WGI is no longer required.

A variation of this formulation also exists where library cross-correlation functions at all ranges and angles can be estimated using a single measurement of acoustic intensity on a single hydrophone recorded from a library vessel in a known position. The intensity function is modified in range using the WGI, and the cross-correlation function across the pair of phones is estimated by multiplying the frequency-shifted intensity function by a complex exponential

$$C(R + \Delta R, \theta) = I(R, \omega + \Delta\omega) e^{2i\bar{k}d\cos(\theta)}, \quad (6)$$

where $I(R, \omega + \Delta\omega)$ is the intensity function, frequency shifted by some $\Delta\omega$ as determined using the WGI for the desired range shift Δr . The derivation of this variation to the formulation is also included in the appendix. This method is advantageous because a single hydrophone can calibrate a region, and populate the full grid with measured cross-correlation replica functions. It is often the case that, in the presence of a potential library vessel, only one hydrophone records a good signal with sufficient SNR, and as a result, the library cross-correlation function cannot be computed. When this is the case, the formulation in Eq. (6) can be used to estimate a library cross-correlation function and create a more densely populated library.

B. Generating the localization ambiguity surface

Once the library of measured replicas is fully populated, an ambiguity surface is generated to show the results of the localization method. The ambiguity surface is generated by computing the correlation coefficient (C_{el}) between the envelope of the normalized time domain library cross-correlation function at every point in the grid (C_l) computed by taking the absolute value of the Hilbert transform of the cross-correlation function and the envelope of the normalized cross-correlation function computed during the passage of the “target” or “event” vessel (C_e),

$$\int C_l(\tau) C_e(\tau) d\tau = C_{el}, \quad (7)$$

where τ is correlation lag time in seconds.

The envelope, or absolute value of the Hilbert transform of the cross-correlation waveforms is used for comparison instead of the cross-correlation waveforms themselves because the differing spectral content of the library and event vessels can cause minor differences in the structure of the cross-correlation waveform, which is smoothed over in the Hilbert transform. Different methods of pre-whitening the signals could be used in place of the Hilbert transform to account for this, without sacrificing the precision in the localization results that is a consequence of using a Hilbert transform, but here the Hilbert transform is employed for robustness. The cross-correlation functions are normalized by the autocorrelation of the signals on each hydrophone. The magnitude of the correlation coefficient between the two envelopes is the value plotted in the ambiguity surface. There are a number of methods that may be used to compare the data and replica cross-correlation functions; the correlation coefficient is the comparison metric presented here.

Each library vessel position with a corresponding measured cross-correlation replica function can be used to fully populate a grid with extrapolated cross-correlation functions. In the example in Sec. IV, seven individual libraries are used, which means there are seven completely populated grids, and the ambiguity surface described above is computed for each of these grids. These ambiguity surfaces are then combined with an inverse distance weighted (IDW) average based on the how far each of the original library cross-correlation functions had to be extrapolated in range. The final ambiguity surface used for localization is

$$C_{eL} = \frac{1}{N} \sum C_{el_n} W_n, \quad (8)$$

where C_{eL} is the final summed ambiguity surface, N is the number of libraries that are being averaged, C_{el_n} represents each of the library grids or surfaces being summed, and W_n is a Gaussian weighting matrix for the n th library,

$$W_n = e^{-\Delta r_n^2 / 2\sigma^2}, \quad (9)$$

where Δr is the difference in range between the grid point in the ambiguity surface and the original library, and σ is the standard deviation of a Gaussian-like curve that describes

the inverse distance weighting surface. In other words, each library grid has an influence on the final ambiguity surface that is weighted based on the inverse-distance the library was extrapolated to each point in the grid. The closest library has the greatest influence on the final result.

III. SIMULATIONS

Simulations are first used to test the localization method by using the normal mode propagation model formulation described in Jensen *et al.*¹⁰ with an input environment very similar to the acoustic environment off the coast of southern California. A grid was selected approximately 5–15 km away from a simulated array in a 150 m deep, downward refracting, range independent acoustic environment. The two hydrophones were spaced 511 m apart. The parameters were chosen to mimic that of the acoustic experiment described in Sec. IV.

In order to test the method using a simulation, a fully populated library was simulated using a broadband acoustic radiator at every position in the grid shown in Fig. 3(a), then cross-correlating those signals and saving the cross-correlation function with the associated latitude and longitude of the simulated contact. The library used to generate the localization results shown in Fig. 3(b) was populated using the extrapolation method described in Sec. II A, Eq. (1). The black \times 's represents the location of ships simulated using the normal mode propagation model. The remainder of the library, 20 degrees to the left and right of each simulated ship's position, and 1.5 km radially closer to the array and further from the array, was populated by modifying the frequency-domain cross-correlation functions using the formulation described in Sec. II A, and Eq. (1). Figure 3(c) is

very similar, but the library is populated using the acoustic intensity on a single hydrophone for a source in a given location, extrapolated in range and angle according the formulation in Eq. (6).

The ambiguity surfaces shown in Fig. 3 were generated (fully populated and extrapolated libraries) by comparing all of the envelopes of the library cross-correlation functions to the envelopes of the cross-correlations computed for a simulated source in a certain location plotted as the grey “+,” using a correlation coefficient. The color that is plotted in the ambiguity surfaces in Fig. 3 is the correlation coefficient for the envelope of each replica correlation function and the “data” correlation function. In other source localization literature, ambiguity surfaces such as those shown in Fig. 3 are often plotted in dB, with a significant dynamic range, whereas these surfaces are plotted on a linear scale from −1 to 1 because they represent the normalized correlation coefficient. This is necessarily a relatively small dynamic range compared to many localization methods but the relative peaks are discernible and allow for continuous tracking. The dynamic range can be increased by not normalizing the correlation coefficients, and plotting the results in dB. There is some ambiguity; however, this can be reduced with averaging the ambiguity surfaces of multiple libraries as presented here, or using multiple combinations of hydrophones. The dynamic range does not increase my averaging multiple libraries, but the uniqueness of the localization does, as each library localizes the contact in the same place, but has different side-lobes and false detections. Each case (fully populated and extrapolated libraries) performs nearly identically in this simplified simulated environment, with approximately equal dynamic ranges on the ambiguity surfaces. It is

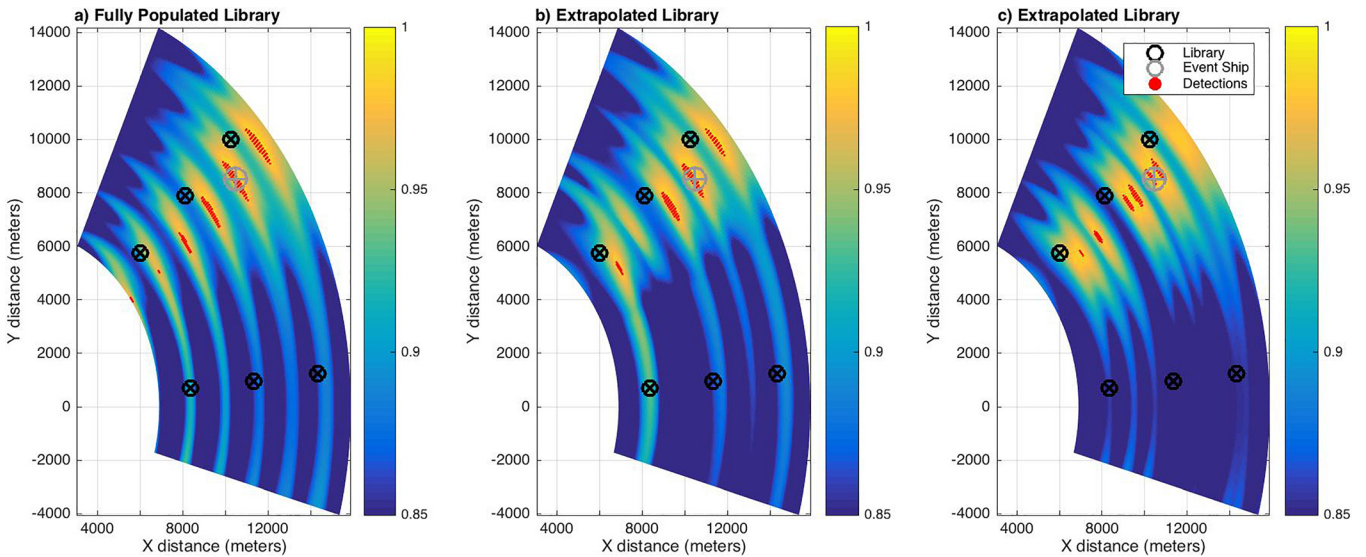


FIG. 3. (Color online) Modeled localization results. (a) is the ambiguity surface generated using a fully populated library of measured replica cross-correlation functions, simulated for every point in the grid and compared to the cross-correlation function of a simulated contact in the position represented by the grey “+.” The color in the ambiguity surface represents the correlation coefficient between the envelope of each library cross-correlation function and the envelope of the “event” cross-correlation function. (b) is a similar ambiguity surface, but the library of replica cross-correlation functions was populated using the formulation in Sec. II A, Eq. (1), extrapolating a single measured cross-correlation function in range and angle. A measured (simulated) cross-correlation function at the position indicated by the black “ \times ” was extrapolated to every point in the grid, and those extrapolated cross-correlation functions were compared to the “event” function. The library of replica functions used to generate the ambiguity surface in (c) was populated using the formulation in Eq. (6); estimating the cross-correlation functions for every point in the grid using the acoustic intensity on a single phone computed for a source at the position indicated by the black “ \times .” In each plot, red dots represent detections, or areas where the ambiguity surface is within one percent of the global maximum.

important to note that these simulations were conducted in range independent environments, with no bathymetry. More unique environments yield more complex acoustic propagation, leading to arrival structures on the hydrophones with more geographic uniqueness. In other words, the method works better in range dependent environments and results from field experiments often outperform simulations conducted in simple range independent environments as long as the variability of the WGI values over the search grid can be estimated *a priori*. In these more complex environments, the extrapolated cross-correlation function libraries shown in Fig. 3(b) start to outperform the extrapolated intensity function libraries shown in Fig. 3(c).

IV. EXPERIMENTAL RESULTS

After exploring the method using numerical simulations, it was tested using data from a field experiment conducted in 2009. The experiment involved a ten-day deployment of four VLAs approximately 20 km off the coast of San Diego, CA. The VLAs each consisted of 16 elements regularly spaced one meter apart, starting approximately 7 m off the

bottom. They were deployed in water approximately 155 m deep, and were spaced approximately 500, 1000, and 1500 m apart. One element from each of two VLAs spaced 511 m apart and positioned approximately 18 m off the bottom was selected for this demonstration. The VLAs sampled at 25 kHz, but the data was down-sampled to 1 kHz, and band-pass filtered between 20 and 300 Hz. Ships were tracked during the entire ten-day experiment using the AIS; the tracking data was obtained upon request from the USCG NAVCEN Nationwide Automatic Identification System (NAIS) database.

Figure 1 shows a plot of the geometry of the experiment. There are three ship tracks transecting the localization grid outlined in black lines in Fig. 1(c). Ship 1 and Ship 2 plotted in green and orange, respectively, in Fig. 1(c), were used to construct the library of measured replicas. The magenta line represents the target ship, not contained in the library data, to be localized using the method. The library ships and event ship have different spectral signatures as can be seen from the spectrograms in Figs. 4(d), 4(e), and 4(f). For each of these vessel tracks, cross-correlations are computed using 0.5 s long snapshots of the data recorded on each of the

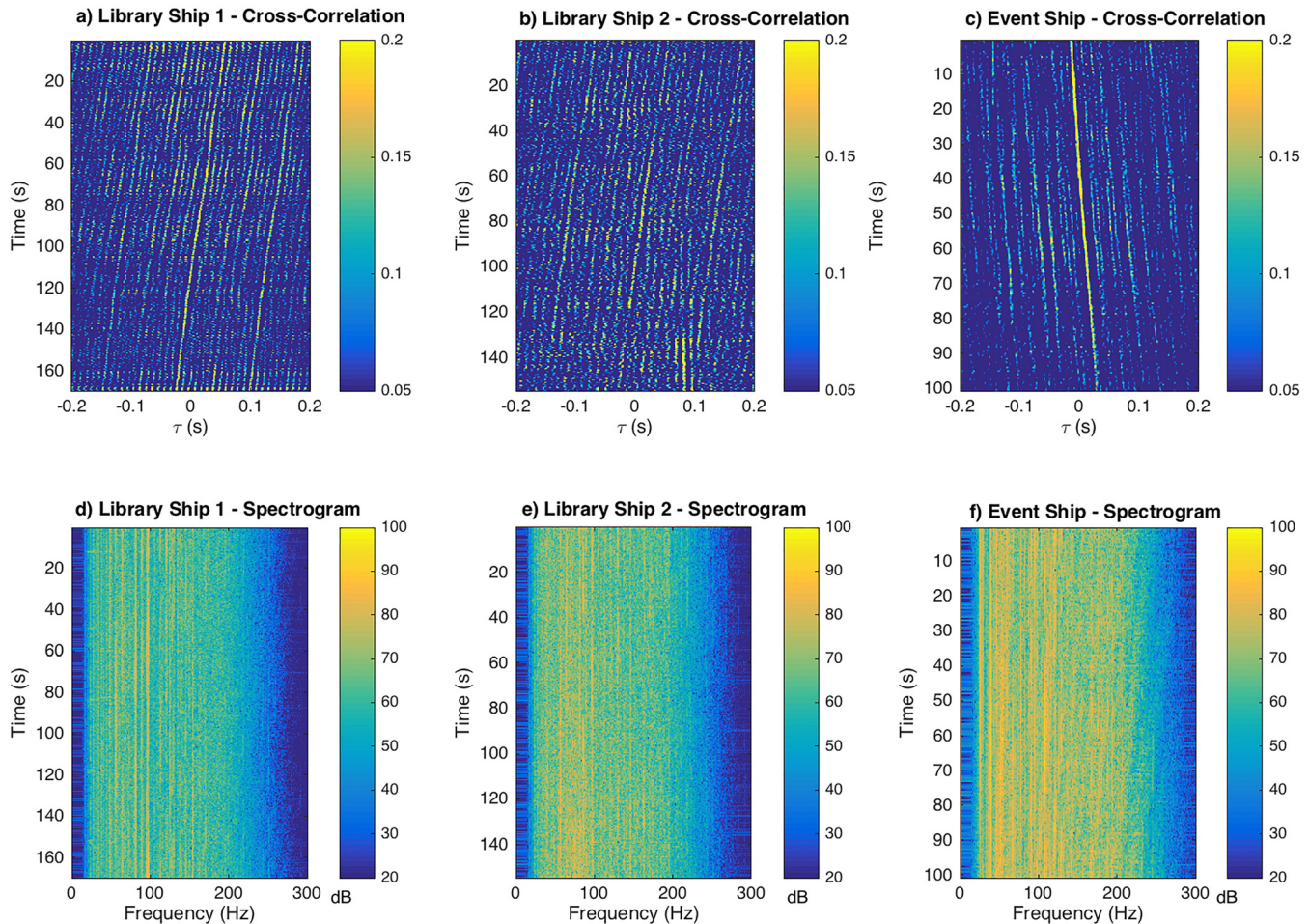


FIG. 4. (Color online) (a) shows the time varying cross-correlation function, normalized by the autocorrelations between the two hydrophones, computed along the track of Library Vessel 1 [the green track in Fig. 1(c)]. Correlation time, τ , is plotted on the x -axis and time along the vessels track is plotted on the y -axis. For the purposes of this demonstration, the signals were band-pass filtered between 20 and 300 Hz, and cross-correlations were computed using 0.5 s long snapshots of the data recorded on each of the receivers. Similarly, (b) and (c) show the same information but for Library Vessel 2 and the “event” vessel (the target vessel to be localized). (d), (e), and (f) are the spectrograms for each of these vessels at the time the cross-correlations were computed with frequency on the x -axis and time along the vessel track on the y -axis.

receivers at every point along the vessels track. These time varying cross-correlation functions are plotted in Figs. 4(a), 4(b), and 4(c). While consistent peaks are present where one would expect for a ship along the track of each vessel, in Figs. 4(a) and 4(b), the peaks are not as easy to discern as in Fig. 4(c). Figure 4(c) represents a better, more strongly correlated ship track; the method performs best when the signals are strongly correlated so this demonstration is less than ideal. Nevertheless, the method functions. Library Ship 1 and 2, were both the R/V NEW HORIZON moving from north to south across the grid, on two different days, five days apart. The “event” ship was a tug and tow that transited from east to west across the experiment site on a day in the middle of this time period.

When the library cross-correlation functions created using the extrapolation method described in Sec. II A are plotted for every point along the event ship track alongside the actual measured cross-correlation function computed along the event ship track as in Fig. 5, it is clear that the extrapolation method is capturing the structure of the cross-correlation function in all locations. Seven discrete locations along the path of two library vessels were selected as “library” cross-correlation functions. These “library” functions were extrapolated to every point in the search grid, and the time varying cross-correlation functions from every point

along the track of the “event” vessel are extracted from that grid and are plotted for three of these libraries in Fig. 5 alongside the computed cross-correlation function along the track of the “event” vessel.

Several discrete locations along the tracks of the library vessels, represented by the black \times 's in Fig. 6(d) are selected as library points. The cross-correlation functions computed when the vessel was in that location, horizontal slices through Figs. 4(a) and 4(b), are extrapolated to all the points within the grid using the formulation in Eq. (1). A smaller search grid is used for the experimental data than the simulation due to the availability of library vessels during the experiment. Then, each of those points are used to generate a fully populated library of estimated replica cross-correlation functions. The envelopes of each of these extrapolated cross-correlation functions are correlated with the envelope of the event cross-correlation function and the correlation coefficient at every point in the grid is plotted in Figs. 6(a), 6(b), and 6(c), representing the ambiguity surfaces for three of the seven libraries generated for this demonstration of the method. These surfaces are combined using an IDW average, preferentially weighting the libraries that have been extrapolated the least distance using the formulation in Sec. II B. This surface is plotted in Fig. 6(d). The locations of the local maxima, defined as points with a correlation coefficient

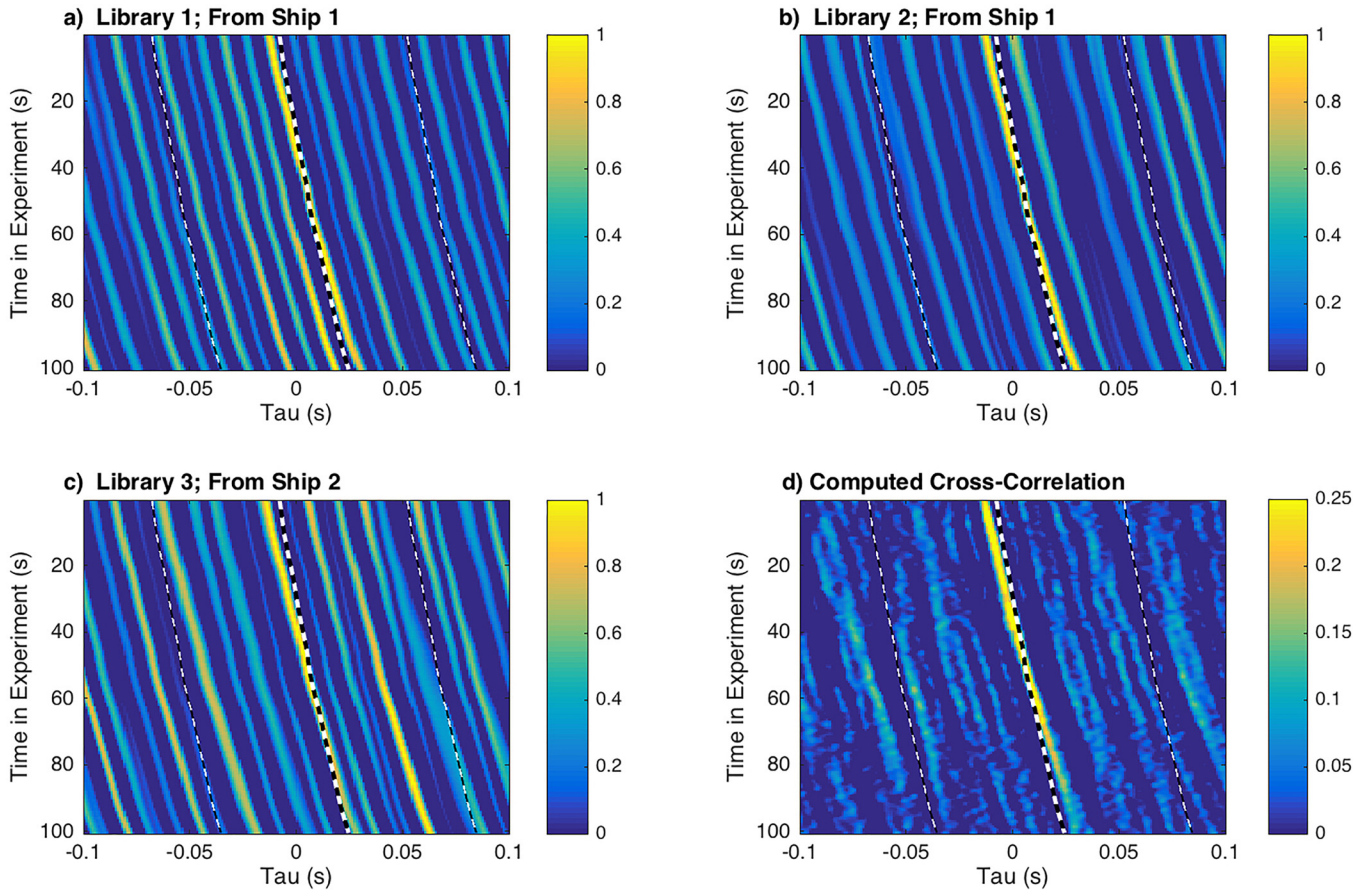


FIG. 5. (Color online) (a), (b), and (c) are the extrapolated time-varying cross-correlation functions taken from the same three libraries used for the experimental localization results. Correlation time, τ , is plotted on the x -axis and time along the vessel's track is plotted on the y -axis. The actual cross-correlation function along the “event” vessel track is plotted in (d). The functions plotted in (a), (b), and (c) are similar to the measured function plotted in (d), which means the extrapolation formulation is doing a reasonable job approximating the cross-correlation at these positions. The black and white lines in each plot represent the theoretical peak lag time across the two phones, and the window of the correlation function used for the comparison.

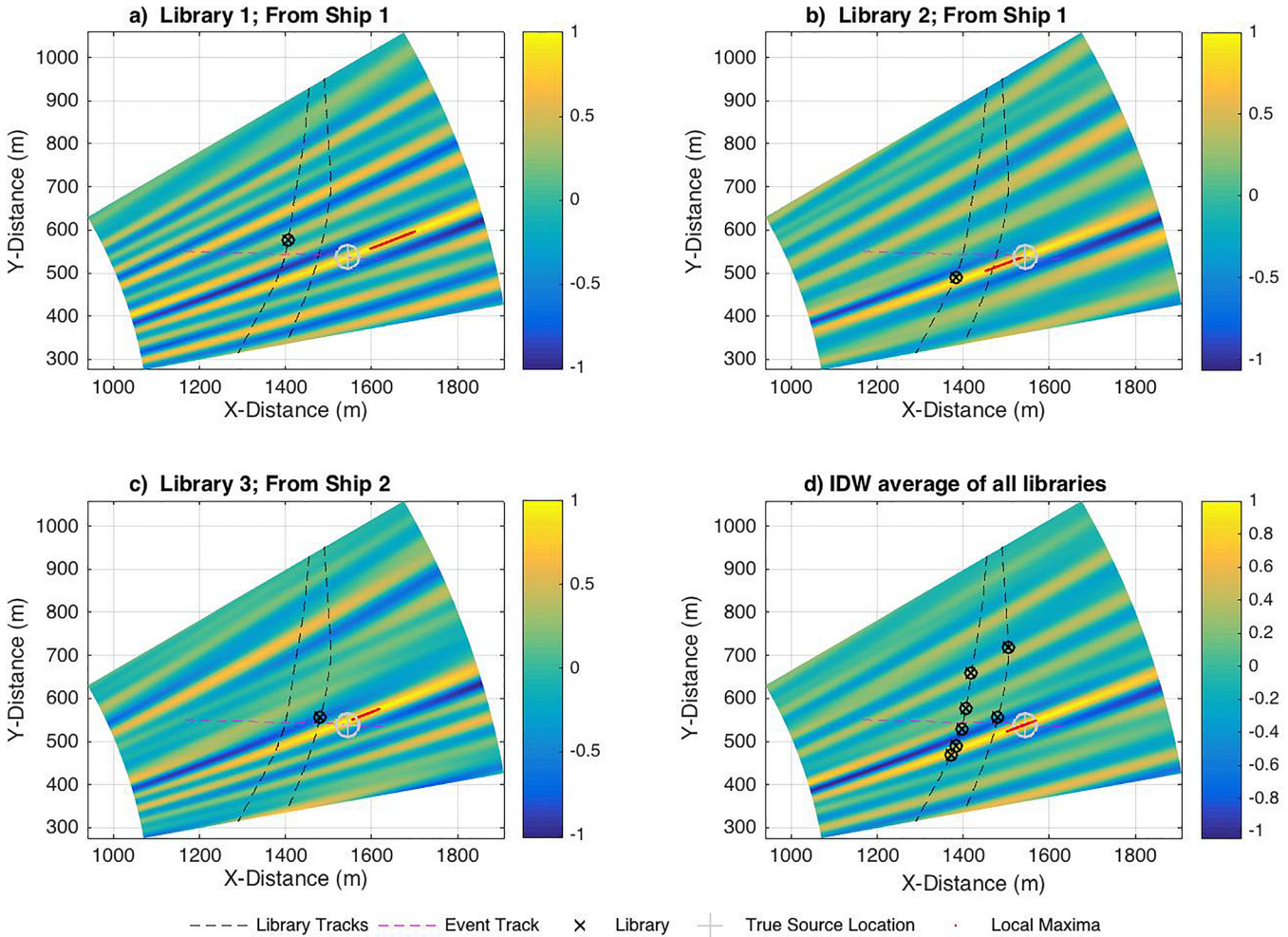


FIG. 6. (Color online) Localization results. (a), (b), and (c) show the ambiguity surface for three library points shown as black “ \times ’s” generated using the formulation in Sec. II B. (d) is the IDW average ambiguity surface computed using the formulation in Sec. II B for the seven library points plotted as black “ \times ’s.” In all cases, the same cross-correlation time interval (-0.2 to 0.2 s) is used. While in every snap shot the averaged surface does not necessarily look better, the results are more consistent and the track that is derived from this surface is far better than from any single library. In each plot, the red dots represent the locations of the local maxima, defined as values in the ambiguity surface within 1% of the value of the global maximum of the surface, and can be thought of as positive “detections.” The grey crosshairs show the “true” position of the target vessel.

within 1% of the global maximum of the surface, are plotted as red dots. There is some ambiguity in range, but the method does accurately localize the target vessel at all points along the vessel’s track. The ambiguity in range decreases when the method is applied at greater ranges in simulation, but the data was limited in this implementation to close ranges. Interestingly, the localization results from experimental data often outperform the modeled results owing to the environmental complexity of the range dependent geometry of the waveguide, creating a more diverse set of unique replica cross-correlation functions.

As with any localization method, side lobes and ambiguity can lead false detections. One of the benefits to this method over the work of Verlinden *et al.*² is the fully populated libraries allow for continuous tracking. If the ambiguity surfaces are generated for every point along the event ship track, and the local maxima (plotted as red dots in Fig. 6) are plotted on the x - y plane with the color of the points representing the time along the track as in Fig. 7(a) it is clear that, while there are outliers, there is a discernible path. The standard error of all the detections, defined as points in the

ambiguity surface having a correlation coefficient within 1% of the global maximum of the ambiguity surface in Fig. 6(d) was 175.1 m. When a simple three-dimensional, iterative, regression-based tracking algorithm is applied to the dataset, the precision of the localization result improves dramatically to a standard error of 24.7 m. The tracking algorithm is not the focus of this study and any number of tracking algorithms, such as a Kalman filter, could be applied. In this demonstration, the tracking algorithm used involved calculating a best fit line through the detections in x - y - t space, eliminating detections that fell outside a certain threshold from that line, recomputing a best fit line, and repeating this process until the standard error is no longer reduced. In this case, the threshold used to eliminate detections was 0.6 standard deviations from the best fit line, with time in seconds weighted $10 \times$ distance in meters. Figure 7(b) shows the results of the tracking algorithm. The actual path that the event ship took is plotted as a magenta line; the locations of each detection are plotted as colored dots, with the color corresponding to time along the vessel’s track, and the black line shows the best fit track resulting from the tracking

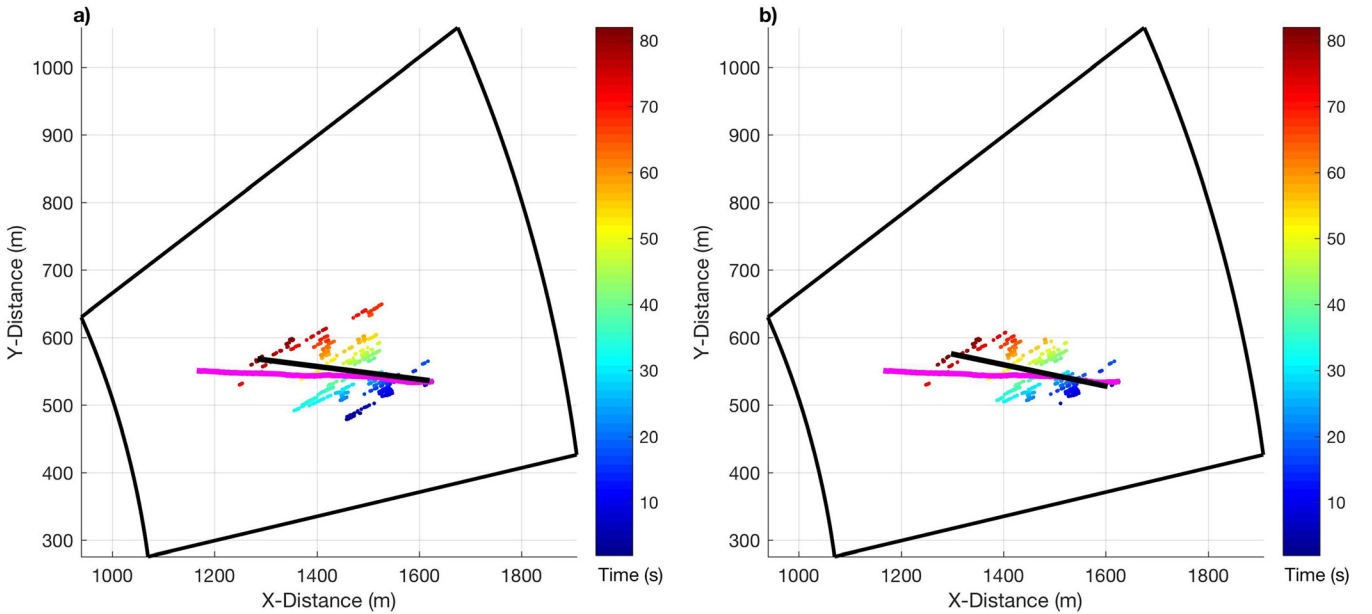


FIG. 7. (Color online) (a) shows all of the “detections” from the ambiguity surface shown in Fig. 6(d) along the track of the “event” vessel plotted on the x - y plane with the color of the dot representing the time along the track in seconds. The true track of the vessel is shown in magenta, while the detected track is shown in black. It is clear that there is a track that follows along the points but there are outliers. (b) shows the detections once the tracking algorithm had been applied and all points along the track that deviated from a three-dimensional regressive best fit line to the data points in (a) are removed. The standard error of the resulting track in (b) is 24.65 m, which represents a considerable improvement over the track in (a), which has a standard error of 175.1 m, for contacts approximately 2 km from the array.

algorithm. There is good agreement between the vessel track and results of the localization method.

While the method performs well in this demonstration, it is sensitive to mismatch in the parameters used in the extrapolation, β , \bar{k} , and \bar{s} . Small changes in these three parameters can lead to error in the resulting localization method in angle and range, depending on the geometry of the experiment. This sensitivity was modeled for the geometry of the simulated localization results shown in Fig. 3, for a contact approximately 12 km away, 45 degrees from array end fire, for hydrophones spaced 500 m apart. The simulated contact is localized using a library extrapolated 750 m in range, and 5 degrees in angle. Small errors in β result in significant errors in range localization. For example, introducing 1% error in β results in a 10 m error in source range, or approximately 1.3% of the extrapolated range, and virtually no error in source azimuth. A 10% mismatch in β yields 75 m error in source range, or approximately 10% the extrapolated range, and approximately 0.2 degrees error in source azimuth or 4% of the extrapolated angle. Introducing an error in \bar{k} has very little impact on source range, but a significant impact on angle. A 1% error in \bar{k} gives virtually no error in range, but approximately 0.1 degrees error in angle or 2% of the extrapolated angle. A 10% error in \bar{k} yields 10 m error in range or approximately 1.3%, and approximately 0.5 degrees error in angle or 10% of the extrapolated angle. The method is comparatively less sensitive to mismatch in \bar{s} with 10% error in \bar{s} yielding virtually no error in range, and only about 0.1 degrees error in angle or 2% of the extrapolated angle. It is important to correctly estimate β and \bar{k} in order to achieve accurate localization results using this method.

In Sec. II A, Eq. (6), an alternative method of estimating library cross-correlation functions, is derived, that involved

using the acoustic intensity function on a single phone to approximate the cross-correlation function across a pair of hydrophones. The results of this method are simulated in Fig. 3(c); performance in field experiments is as predicted.

V. ENVIRONMENTAL ROBUSTNESS

The cross-correlation functions that are used in this method to localize contacts derive their uniqueness from the geoacoustic and physical oceanographic environment. The physical oceanographic environment is non-stationary, and changes with seasonal and diurnal heating-cooling as well as with the passage of internal waves. If the waveguide changes sufficiently between when the library cross-correlation function was computed and the passage of the ship one is attempting to localize, it stands to reason that the library cross-correlation function will no longer be representative of a particular location within the waveguide and the method could break down. In areas with heavy ship traffic, libraries can be constantly renewed with up to date measured replicas, but it is valuable to know how often this must be done. In deep water, and at high frequencies where the acoustic propagation is strongly dependent on water properties, this is a concern. This experiment was conducted in sufficiently shallow water and at frequencies low enough that the arrival structure was primarily a function of the geoacoustic environment (i.e., bottom properties and bathymetry), so this was not a concern. During the experiment, measured replicas were used to localize contacts up to seven days later at any time of day and during different stages in the tidal cycle. Figure 8 illustrates the tolerance of this method to the stationarity of the sound speed profile by showing the results of the localization method using fully

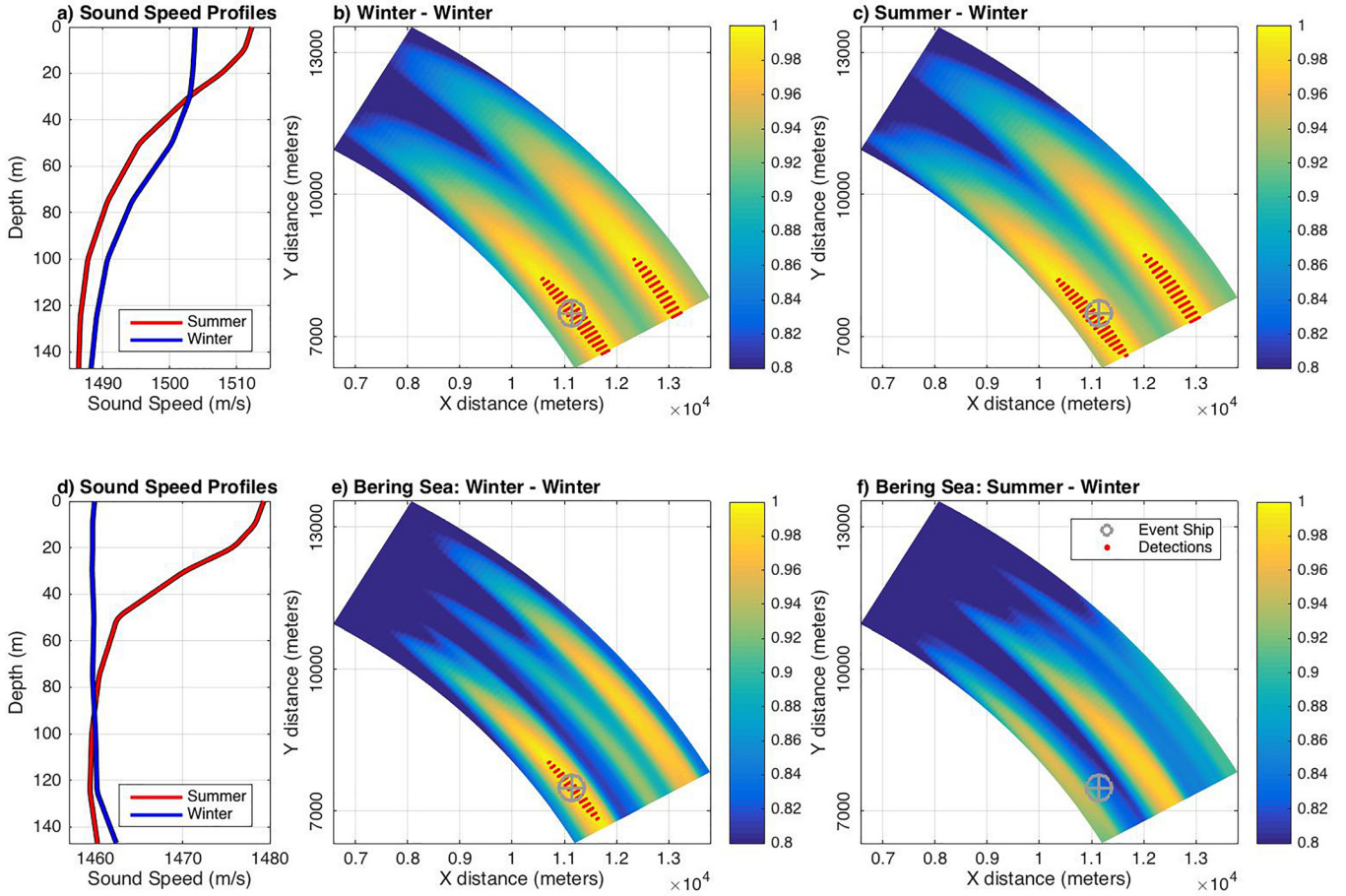


FIG. 8. (Color online) (a) shows a typical sound speed profile for the experiment site taken from the WOA for summer (red) and winter (blue). When a winter profile is used to generate the simulated cross-correlation functions used to create the library and the event cross-correlation functions, the method works as before, as shown in (b), with positive detections shown in red. When a winter profile is used to simulate the library replicas, but a summer profile is used to simulate the event cross-correlation function, the method still performs acceptably well in this environment (error less than 20 m), as shown in (c). (d) shows typical summer and winter sound speed profiles taken from WOA for the Bering Sea. (e) shows the results of the localization method when the library and event correlation functions are both generated with the winter profile, while (f) shows the results of the method when a winter library is used to localize a summer event ship. Here the method does not perform well (error over 100 m) due to the significant difference between the summer and winter sound speed profiles.

populated (i.e., non-extrapolated) libraries of replica cross-correlation functions in a small search grid in order to visualize small errors in the localization method which result from changes in the sound speed profile.

In order to demonstrate this principle, an average climatological sound speed profile for the region during the winter taken from the World Ocean Atlas (WOA)¹³ was used to create a library of replicas using a standard normal mode propagation model, and this library was then used to localize a contact with a signal that was simulated using the same propagation model but using an average climatological summer sound speed profile. This was designed to show how the method would behave under the most different of possible physical oceanographic environments for the region. Figure 8(a) shows the two sound speed profiles; winter (blue) used to generate the library of replicas; summer (red) used to generate the source signal of the contact to be localized. Figure 8(b) shows the localization result when the two profiles are the same, both winter; and Fig. 8(c) shows the results when the winter library is used to localize the summer target. Performance of the method degrades with error in the localization results of 20 m, but does not entirely break down.

This means that the library cross-correlation functions do not have an expiration date in this environment, but this will not be true in all environments. For example, in the Bering Sea, a region of comparable depth, the sound speed profile changes more dramatically from strongly downward refracting in the summer to isovelocity or even upward refracting in the winter. A standard summer and winter sound speed profile are taken from the WOA and are plotted in Fig. 8(d). The localization method works when the sound speed profile from the library matches the event as is the case in Fig. 8(e), but when a winter sound speed profile is used to generate the library, and that library is used to localize an event simulated using a summer profile, the method does not perform as well as shown in Fig. 8(f) with errors over 100 m. There is still a large peak in the correlation coefficient ambiguity surface, but it is offset significantly in range, and slightly offset in azimuth. This is consistent with errors in β , \bar{k} , and \bar{s} values used to extrapolate the library, which is expected given the change in surface sound speed. It is likely that this change can be accounted for by modifying the β , \bar{k} , and \bar{s} values used to construct the extrapolated cross-correlation function library as is sometimes done in MFP.¹ Additionally, by

nature of the library being populated with sources of opportunity, it will necessarily be continually refreshed as ships continue to transit the region, eliminating the issue of seasonal expiration of measured replicas in certain areas, and diminishing the need to modify existing libraries of measured replicas.

VI. CONCLUSION

It is possible to localize an acoustic radiator at any position in the marine environment using a library of replica cross-correlation functions, estimated by extrapolating existing measured cross-correlation functions to different angles and ranges, using WGI theory. The spatial uniqueness of the library is enhanced in complex, range dependent marine environments. The fully populated library allows for continuous tracking, which improves localization results. In some highly dynamic environments, the method is sensitive to non-stationarity of the sound speed profile.

There are a number of signal processing techniques that could be used to optimize and improve the results of this localization method. Various methods of pre-whitening and normalizing replica cross-correlation functions including the use of a Smoothed Coherence Transform¹⁴ and cross-coherence functions¹⁵ will likely improve performance in localizing sources that have vastly different source spectra than those used to construct the library.

Areas for future research include employing combinations of hydrophones or arrays of hydrophones in constructing the correlation libraries, along with experimenting with different array geometries may optimize results. Averaging ambiguity surfaces from multiple combinations of hydrophones improves localization results and reduces spatial ambiguity. Cross-correlating beams taken from vertical arrays will improve the uniqueness of the cross-correlation functions used for localization. Cross-correlating broadside beams on horizontally separated VLAs will likely emphasize mode one arrivals and make it possible to localize a sub-surface contact with a surface derived library. It is possible that this method could be expanded to localize subsurface sources using a library derived from surface sources, by modifying β , \bar{k} , and \bar{s} values used to construct the extrapolated libraries. Library cross-correlation functions can also likely be modified to account for seasonal changes in the sound speed profiles in order to account for the non-stationary nature of the ocean waveguide.

Additional experimental verification is required in different marine environments. Further study may include an experiment in deeper water (500–700 m) with longer propagation paths to investigate how robust the method is to physical oceanographic complexity. Ideally, an experiment site with high vessel traffic density will be selected so the library of measured replicas can be more densely populated than in this demonstration, allowing for the exploration of different methods for combining multiple libraries for a single localization result.

ACKNOWLEDGMENTS

This work was supported by the Office of Naval Research.

APPENDIX

1. Extrapolation derivation

Measured library replica cross-correlation functions can be modified in range and angle to fully populate a search grid allowing for continuous tracking by frequency-shifting the cross-correlation function according to WGI theory, and multiplying it by a complex exponential term derived here.

It is helpful to start from the standard normal mode approximation for the cross-correlation function across two hydrophones,¹⁰

$$C_{12}(R, \theta) = (P(r_1)P^*(r_2))_0 \\ = \sum a_{nm} e^{i(k_n - k_m)R} e^{i(k_n + k_m)d \cos \theta}. \quad (\text{A1})$$

To extend this in both angle and range, an approximation for $C_{12}(R + \Delta r, \theta + \Delta \theta)$ must be derived so R is replaced with $R + \Delta r$, and θ is replaced with $\theta + \Delta \theta$,

$$C_{12}(R + \Delta r, \theta + \Delta \theta) \\ = \sum a_{nm} e^{i(k_n - k_m)(R + \Delta r)} e^{i(k_n + k_m)d \cos(\theta + \Delta \theta)}.$$

First, the $(R + \Delta r)$ in the first exponential can be accounted for with standard WGI theory where

$$(k'_n - k'_m)(R) = (k_n - k_m)(R + \Delta r),$$

and k'_n and k'_m are the horizontal modal wavenumbers shifted by some frequency $\Delta\omega$ corresponding to the Δr in accordance with WGI theory,

$$k'_n = k_n(\omega + \Delta\omega), \\ k'_m = k_m(\omega + \Delta\omega).$$

Thus, the $e^{i(k_n - k_m)(R + \Delta r)}$ term becomes $e^{i(k'_n - k'_m)R}$. Expanding k'_n about k_n yields

$$k'_n = k_n(\omega + \Delta\omega) = k_n(\omega) + \frac{dk_n}{d\omega} \Delta\omega,$$

which means that

$$(k'_n + k'_m)d \cos(\theta + \Delta \theta) \\ = \left(\left(k_n(\omega) + \frac{dk_n}{d\omega} \Delta\omega \right) + \left(k_m(\omega) + \frac{dk_m}{d\omega} \Delta\omega \right) \right) \\ \times d \cos(\theta + \Delta \theta),$$

which with some rearranging becomes

$$(k_n + k_m)d \cos(\theta + \Delta \theta) = (k'_n + k'_m)d \cos(\theta + \Delta \theta) \\ - \left(\frac{dk_n}{d\omega} + \frac{dk_m}{d\omega} \right) \Delta\omega d \cos(\theta + \Delta \theta).$$

So the $e^{i(k_n + k_m)d \cos(\theta + \Delta \theta)}$ term becomes $e^{i(k'_n + k'_m)d \cos(\theta + \Delta \theta)} \times e^{-i(dk_n/d\omega + dk_m/d\omega)\Delta\omega d \cos(\theta + \Delta \theta)}$, and

$$C_{12}(R + \Delta r, \theta + \Delta \theta) = \sum a_{nm} e^{i(k'_n - k'_m)R} e^{i(k'_n + k'_m)d \cos(\theta + \Delta \theta)} \\ \times e^{-i(dk_n/d\omega + dk_m/d\omega)\Delta\omega d \cos(\theta + \Delta \theta)}.$$

Now using trigonometric identities,

$$\cos(\theta + \Delta\theta) = \cos(\theta)\cos(\Delta\theta) - \sin(\theta)\sin(\Delta\theta),$$

and for small $\Delta\theta$ s, $\cos(\Delta\theta) \rightarrow 1$ and $\sin(\Delta\theta) \rightarrow \Delta\theta$, so the expression becomes

$$\cos(\theta + \Delta\theta) = \cos(\theta) - \sin(\theta)\Delta\theta.$$

Thus, the $e^{i(k'_n+k'_m)d\cos(\theta+\Delta\theta)}$ term becomes $e^{i(k'_n+k'_m)d(\cos(\theta)-\Delta\theta\sin(\theta))}$, and the entire expression simplifies to

$$C_{12}(R + \Delta r, \theta + \Delta\theta) = \sum a_{nm} e^{i(k'_n-k'_m)R} e^{i(k'_n+k'_m)d(\cos(\theta)-\Delta\theta\sin(\theta))} \times e^{-i(dk_n/d\omega+dk_m/dk_n)\Delta\omega d\cos(\theta+\Delta\theta)}$$

which with some rearranging becomes

$$C_{12}(R + \Delta r, \theta + \Delta\theta) = \sum a_{nm} e^{i(k'_n-k'_m)R} e^{i(k'_n+k'_m)d\cos(\theta)} e^{-i(k'_n+k'_m)\Delta\theta\sin(\theta)} \times e^{-i(dk_n/d\omega+dk_m/dk_n)\Delta\omega d\cos(\theta+\Delta\theta)}.$$

According to WGI theory, $\sum a_{nm} e^{i(k'_n-k'_m)R} \times e^{i(k'_n+k'_m)d\cos(\theta)} = C_{12}(R, \theta, \omega + \Delta\omega)$; in other words, the original cross-correlation function frequency shifted by some $\Delta\omega$ corresponding the Δr you desire to range shift the function. Then we introduce the average wavenumber term \bar{k} , where $\bar{k} = \frac{1}{2}(k_n + k_m)$; as well as an average modal group slowness term \bar{s} . Since modal group speed $u_n = d\omega/dk_n$,

$$\frac{dk_n}{d\omega} + \frac{dk_m}{d\omega} \approx 2\bar{s},$$

where \bar{s} is the average modal group slowness or the reciprocal of modal group speed. Substituting \bar{k} and \bar{s} into the expression for the extrapolated cross-correlation function, the expression for $C_{12}(R + \Delta r, \theta + \Delta\theta)$ becomes

$$C_{12}(R + \Delta r, \theta + \Delta\theta) = C_{12}(R, \theta, \omega + \Delta\omega) e^{-i2\bar{k}\Delta\theta\sin(\theta)} e^{-2\bar{s}\Delta\omega d\cos(\theta+\Delta\theta)}, \quad (\text{A2})$$

which is the formulation from Eq. (1). It is important to note that if the change in range is set equal to zero, then $\Delta\omega$ is zero and the formulation becomes an angle-only extrapolation as in Eq. (5). In other words, if measured replicas exist at all desired ranges (for example, from a radial ship track), then it may only be necessary to extrapolate the measured replicas to other angles. Using this formulation, it is possible to extrapolate a cross-correlation function measured when a ship was in one position to a different range and bearing; which makes it possible to fully populate a region with extrapolated measured cross-correlation replica functions, which can be used for localization and continuous tracking. In simulations, this method was effective up to about 7 degrees. The angle over which the replicas can be extrapolated is limited by the law of cosines approximation in the first section of this derivation and is therefore a function of range from the receivers. It is also limited by the changing bathymetry in the region.

2. Estimating cross-correlation functions from intensity

There is a variation of this formulation that can be used to construct a library of estimated cross-correlation functions from the recorded acoustic intensity on a single hydrophone. This formulation is useful in circumstances where, for whatever reason, measured cross-correlation replica functions do not exist in all desired places, but intensity has been recorded on at least one hydrophone. If, for example, there is only one functional hydrophone in the region, or one of the phones in the array did not receive a clear signal from the library vessel, it is still possible to estimate cross-correlation functions for the library. In many instances during the experiment, this method was useful for creating a more densely sampled search grid of replica cross-correlation functions, which can improve localization results; however, the experimental results are not presented here. It is important to note that, while the library cross-correlation functions are estimated using the following formulation, the data from the target vessel to be localized is still the measured cross-correlation across the two hydrophones in the array.

Beginning with the same normal-mode based expression for the cross-correlation function from before,

$$C(\theta, R) = (P(r_1)P^*(r_2))_\theta = \sum a_{nm} e^{i(k_n-k_m)R} e^{2i\bar{k}d\cos\theta}, \quad (\text{A3})$$

and the formulation for the acoustic intensity on a single phone at a range R ,

$$I(R) = P(R)P^*(R) = \sum a_{nm} e^{i(k_n-k_m)R}, \quad (\text{A4})$$

where I is the acoustic intensity, it is possible to write the expression for a cross-correlation function at a given range R from the array center position and bearing θ off the array azimuth in terms from the intensity of a source at the same range,

$$C(R, \theta) = I(R) e^{2i\bar{k}d\cos(\theta)}. \quad (\text{A5})$$

This means that the cross-correlation function at a certain angle θ and a range where measured replicas do not exist $R + \Delta r$ can be estimated by frequency shifting the intensity function recorded from a source at a known range, by some $\Delta\omega$ associated with the proper shift in range Δr according to the WGI [Eq. (3)],

$$C(R + \Delta r, \theta) = I(R, \omega + \Delta\omega) e^{2i\bar{k}d\cos(\theta)}. \quad (\text{A6})$$

Using this formulation, it is possible to fully populate a library of estimated cross-correlation functions for all ranges and bearings, using intensity from a single hydrophone, frequency shifted using the WGI, and modified using a complex exponential term.

No matter which method is used for fully populating a spatial library with cross-correlation replica functions, once the entire study is populated, it is possible to localize contacts using the methods from Verlinden *et al.*² in all locations and do continuous tracking.

- ¹A. B. Baggeroer, W. A. Kuperman, and P. N. Mikhalevsky, “An overview of matched field methods in ocean acoustics,” *IEEE J. Oceanic Eng.* **18**(4), 401–424 (1993).
- ²C. M. A. Verlinden, J. Sarkar, W. S. Hodgkiss, W. A. Kuperman, and K. G. Sabra, “Passive acoustic source localization using sources of opportunity,” *J. Acoust. Soc. Am.* **138**(1), EL54–EL59 (2015).
- ³L. T. Fialkowski, M. D. Collins, W. A. Kuperman, J. S. Perkins, L. J. Kelly, A. Larsson, J. A. Fawcett, and L. H. Hall, “Matched-field processing using measured replica fields,” *J. Acoust. Soc. Am.* **107**(2), 739–746 (2000).
- ⁴P. Roux and W. A. Kuperman, “Extracting coherent wave fronts from acoustic ambient noise in the ocean,” *J. Acoust. Soc. Am.* **116**(4), 1995–2003 (2004).
- ⁵S. Kim, W. A. Kuperman, W. S. Hodgkiss, H. C. Song, G. F. Edelmann, and T. Akal, “Robust time reversal focusing in the ocean,” *J. Acoust. Soc. Am.* **114**(1), 145–157 (2003).
- ⁶A. M. Thode, “Source ranging with minimal environmental information using a virtual receiver and waveguide invariant theory,” *J. Acoust. Soc. Am.* **108**(4), 1582–1594 (2000).
- ⁷G. A. Grachev and J. S. Wood, “Theory of acoustic field invariants in layered waveguides,” *Acoust. Phys.* **39**(1), 33–35 (1993).
- ⁸S. Chuprova, “Interference structure of the sound field in a stratified ocean,” in *Ocean Acoustics. Current Status*, edited by L. M. Brekhovskikh (Nauka, Moscow, 1982), pp. 71–91 (in Russian).
- ⁹W. A. Kuperman, G. L. D’Spain, H. C. Song, and A. M. Thode, “The generalized waveguide invariant concept with application to vertical arrays in shallow water,” in *Ocean Acoustic Interference Phenomena and Signal Processing* (AIP, College Park, MD, 2002), Vol. 33.
- ¹⁰F. B. Jensen, W. A. Kuperman, M. B. Porter, and H. Schmidt, *Computational Ocean Acoustics* (Springer Science & Business Media, New York, 2011).
- ¹¹G. L. D’Spain and W. A. Kuperman, “Application of waveguide invariants to analysis of spectrograms from shallow water environments that vary in range and azimuth,” *J. Acoust. Soc. Am.* **106**(5), 2454–2468 (1999).
- ¹²C. M. A. Verlinden, J. Sarkar, B. D. Cornuelle, and W. A. Kuperman, “Determination of acoustic waveguide invariant using ships as sources of opportunity in a shallow water marine environment,” *J. Acoust. Soc. Am.* **141**, EL102–EL107 (2017).
- ¹³S. Levitus and T. P. Boyer, “World ocean atlas 1994. Volume 4. Temperature,” Technical Report, National Environmental Satellite, Data, and Information Service, Washington, D.C. (1994).
- ¹⁴G. C. Carter, A. H. Nuttall, and P. G. Cable, “The smoothed coherence transform,” *Proc. IEEE* **61**(10), 1497–1498 (1973).
- ¹⁵M. J. Buckingham, “Cross-correlation in band-limited ocean ambient noise fields,” *J. Acoust. Soc. Am.* **131**(4), 2643–2657 (2012).